AIP Applied Physics Letters

Probing the intrinsic conductivity of multiwalled carbon nanotubes

Mikhail Zamkov, Ali S. Alnaser, Bing Shan, Zenghu Chang, and Patrick Richard

Citation: Appl. Phys. Lett. **89**, 093111 (2006); doi: 10.1063/1.2340537
View online: http://dx.doi.org/10.1063/1.2340537
View Table of Contents: http://apl.aip.org/resource/1/APPLAB/v89/i9
Published by the American Institute of Physics.

Probing the intrinsic conductivity of multiwalled carbon nanotubes

Mikhail Zamkov[a)]
University of Illinois at Urbana-Champaign Urbana, Box 71-6 CLSL, MC 712 600 S. Mathews, Illinois 61801 and James R. Macdonald Laboratory, Department of Physics, Kansas State University, Manhattan, Kansas 66506-2604

Ali S. Alnaser, Bing Shan, Zenghu Chang, and Patrick Richard
James R. Macdonald Laboratory, Department of Physics, Kansas State University, Manhattan, Kansas 66506-2604

(Received 27 March 2006; accepted 20 July 2006; published online 29 August 2006)

The authors report the two-photon electron emission study of quantum transport parameters in multiwalled carbon nanotubes. The present experimental approach is based on measurements of the electron-phonon scattering dynamics and does not employ any electrical contacts, which dramatically reduces the uncertainty in the determination of an electron mean-free path l. It is found that near the Fermi level (<0.1 eV) the ballistic travel of electrons averages around 4 μm, which is comparable to the nanotube length, whereas in high-current regime ($\geqslant 0.3$ eV) l decreases to less than 1 μm. © *2006 American Institute of Physics*. [DOI: 10.1063/1.2340537]

When a multiwalled carbon nanotube (MWCNT) is placed between two electrodes it forms a complex circuit that contains several electronically distinguishable single walled shells each capped by a pair of independent contact loads. The electric current in the system will thus be determined by a set of unknown dissipative elements, causing a convoluted relation between the experimental I-V curves and intrinsic conductivity of a MWCNT. As a result, until now the interpretation of the data observed in transport studies has been posing significant challenges,[1–12] preventing experimentalists from reaching an agreement on the value of an electron mean-free path l, which is a critical parameter in establishing the ballistic aspects of the conductance. In particular, the average value of l is typically determined through an approximate relation $l=h/(2e^2)\times 1/(n\rho)$,[10] which requires the knowledge of the nanotube resistance ρ and the number of participating conducting layers n. Both of these parameters, however, cannot be unambiguously determined in transport studies, owing to large variations in the nanotube-electrode junction resistance (0.1–150 kΩ),[4,11] and the possibility of connecting two electrodes to the two different shells of the MWCNT, in which case hopping between adjacent shells would play a decisive role in carrier transport.[13] Accordingly, the reported experimental values of the electron mean-free path are far from unanimous ranging from 0.1 to 30 μm.[3,6,9–12] In the present study we attempt to overcome these problems by using an alternative experimental approach that does not employ any electrical contacts to a nanotube.

According to Fermi gas formalism, the resistance in metals is determined by inelastic collisions of carriers with impurities and quantized vibrations (phonons). It is the frequency of these collisions that defines the electron mean-free path and ensuing conductivity parameters. In the case of room-temperature MWCNTs, the dominant dissipative process limiting the value of l was shown to be the electron-phonon scattering.[14,15] Accordingly, the associated scattering rate, $1/\tau_{\text{e-ph}}(E)$, will contain the full information on the average collision-free distance, $l_{\text{e-ph}}(E)$, for an electron in a conduction state with energy E. In the present study, the electron-phonon scattering rates are measured by means of two-photon electron emission spectroscopy. This technique, also known as time-resolved photoemission (TRPE), provides a powerful tool for studying relaxation dynamics of charge carriers on the ultrashort time scale and offers an excellent resolution in electron energy. The extraction of electron-phonon (e-ph) decay times, $\tau_{\text{e-ph}}(E)$, from a TRPE signal, however, can be realized only if contributions from other mechanisms of an electron escape from the conduction state, such as e-e scattering is identified and excluded from the analysis. Accordingly, we also investigate the competing processes of state depletion to isolate the correct value of $\tau_{\text{e-ph}}(E)$.

The experimental setup as well as the time-resolved excitation scheme has been described elsewhere.[16,17] Initially, the nanotube sample (15 ± 5 nm diameter, high-purity MWCNT buckypaper[18]) is perturbed by the near IR pump beam with a tunable photon energy of 1.3–1.6 eV, which promotes the electron population from below E_F into the conduction band. The resulting perturbation, consisting of electron-hole (e-h) pairs, is then probed with an UV pulse that energetically exceeds the sample work function by approximately 0.5 eV, delivering information on the lifetime of both the conduction electrons and valence holes.[17] It should be noted that the present approach is based on the assumption that the investigated electronic system is driven out of the equilibrium by the excitation pulse, such that the depletion of a conduction state dominates its population.

The relaxation dynamics of charge carriers was measured in the range of -0.4–3 ps. Figure 1 shows the temporal evolution of the excited electron population (cross-correlation trace) recorded for the states with energies of $E_1=0.17\pm 0.05$ eV and $E_2=0.5\pm 0.05$ eV above E_F. Each curve exhibits two different decay trends that were previously observed and characterized for the case of single walled carbon nanotube (SWCNT) ropes.[17] The initial relaxation, indicated by a fast decay component in Fig. 1, is attributed to the internal thermalization of the electronic system, which is primarily driven by e-e scattering processes.

[a)]Electronic mail: zamkov@uiuc.edu

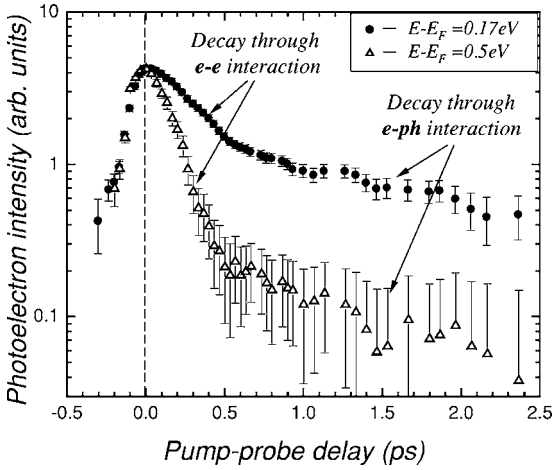

FIG. 1. Experimental cross-correlation traces. The photoemission signal is plotted vs the pump-probe delay for the conduction electrons at $E-E_F=0.17\pm0.02$ eV (solid circles) and $E-E_F=0.5\pm0.02$ eV (open triangles). In both cases, the experimental curve exhibits two easily distinguishable components that are attributed to carrier relaxation through collisions with electrons (fast decay) and phonons (slow decay).

After the system returns to the Fermi-Dirac distribution it continues to decay with a slower rate associated with electron gas cooling by e-ph interactions. We evaluate the individual contributions for the two decay components, $\tau_{\text{e-e}}$ and $\tau_{\text{e-ph}}$, by fitting the experimental data with the convolution of the pump-probe correlation and a biexponential curve. Notably, the characteristic time scales for e-e and e-ph interactions are sufficiently different and thus easy to identify (see Fig. 1). Since the present study focuses on the dynamics of e-ph scattering processes, $\tau_{\text{e-e}}$ is subtracted from the experimental cross-correlation signal and the remaining slow component, $\tau_{\text{e-ph}}$, is investigated.

Figure 2 shows the e-ph scattering times derived from the electron relaxation dynamics in the energy range of 0–0.6 eV above E_F. The experimental uncertainty, denoted by vertical error bars, represents a geometrical sum of the statistical and fitting errors, where the latter is primarily determined by the uncertainty of the exponential fit to the e-ph part of the cross-correlation trace (see Fig. 1). Assuming that near E_F electrons move at a Fermi velocity, $v_F=8\times10^5$ m/s,[15,19] we obtain the electron mean-free path due to e-ph scattering. The overall uncertainty for the determination of the mean-free path through the e-ph decay dynamics is estimated not to exceed 40%, which is a significant improvement over variations in l observed in transport studies. The resulting mean-free paths, shown as an additional Y axis in Fig. 2, exhibit a well-defined dependence on the electron energy. For excitations near the Fermi level, $E-E_F\leqslant0.1$ eV, electrons travel 4 μm on average between successive collisions with phonons, which is comparable to the MWCNT length. The electron relaxation from high-energy conduction bands ($E-E_F\geqslant0.3$ eV) occurs on a slightly shorter time scale (see Fig. 2), which corresponds to the mean-free path of less than 1 μm. Under these conditions, electrons are likely to experience more than one collision with phonons inside a nanotube, indicating that the charge transport in more energetic bands could be diffusive. By assuming that all conductive SWCNT shells participate in the charge transport near E_F we can estimate an effective nanotube resistance using the approximate relation[10] for l (given above) to be 0.4 kΩ/μm.

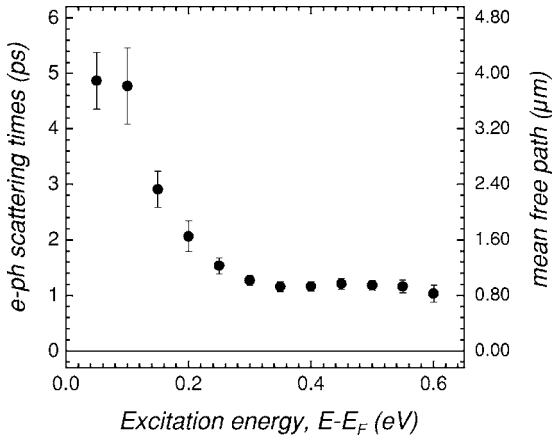

FIG. 2. Experimental e-ph scattering times and the associated electron mean-free paths measured at several electron energies above E_F.

The effect of the laser pump pulse that promotes the large fraction of electrons into the conduction band can be viewed as the increase in the thermal energy of the electronic system. In this case, the thermal equilibrium between the unperturbed lattice and excited carriers will be realized by the energy exchange (cooling) through e-ph interaction. The rate for this energy transfer will contain information on the strength of e-ph coupling, which would allow obtaining an alternative estimate of e-ph scattering times $\tau_{\text{e-ph}}$.

In the framework of the two-temperature model (TTM), adapted for the case of carbon nanotubes,[20] the electron gas temperature can be related to the electron-phonon coupling term $H(T_e,T)$ by

$$C_e\frac{dT_e}{dt}=-H(T_e,T), \tag{1}$$

where $C_e=\gamma T_e$ is the electronic heat capacity (in J/m^3 K). The value of $H(T_e,T)$ determines the instantaneous e-ph energy relaxation time, which, according to TTM, is given by

$$\tau_E(T_e)=\frac{\gamma(T_e^2-T^2)}{2H(T_e,T)}=-\frac{\gamma(T_e^2-T^2)}{2T_e}\left(\frac{dT_e}{dt}\right)^{-1}. \tag{2}$$

We now obtain the e-ph quasiparticle relaxation time, $\tau_{\text{e-ph}}(T_e)$, averaged by $\partial f/\partial E$ over states near E_F, by introducing a temperature-dependent correction to the energy transfer rate,[21]

$$\tau_{\text{e-ph}}(T_e)=\tau_E(T_e)A\frac{1-(T/T_e)^2}{1-(T/T_e)^5}, \tag{3}$$

where $A=0.9534\ldots$.[21] The expression on the left-hand side is independent of the MWCNT specific heat capacity and is determined only by the temporal evolution of the electronic temperature, $T_e(t)$.

Experimentally, $T_e(t)$ can be determined by probing the width of the charge energy distribution near E_F.[22] We note that the change in the electron population at E_F induced by the pump pulse (excitation spectra) should reflect the difference of the distribution functions for the perturbed (T_e) and the initial (T) states of the system. Figure 3(a) shows two examples of the excitation spectra measured for the pump-probe delays of 0.15 and 1.9 ps. The experimental data are fitted with a difference of the distribution functions, $\Delta f=f(T_e)-f(T)$, yielding the corresponding value of T_e for

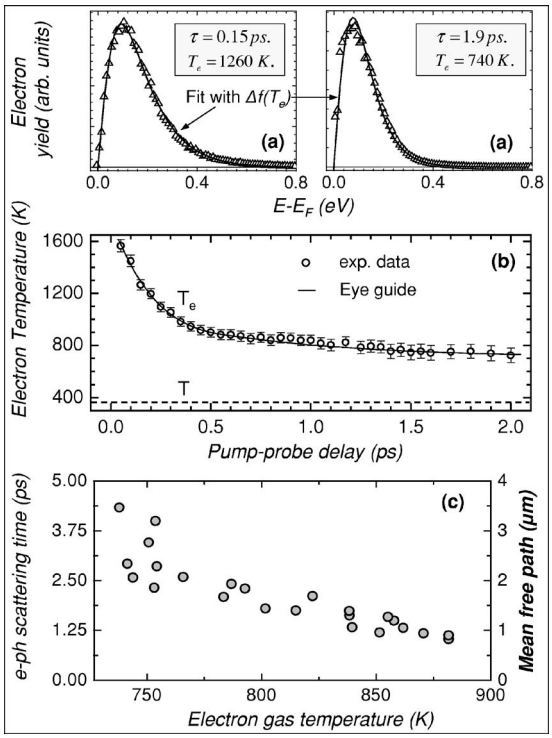

FIG. 3. Cooling of the excited electronic system. (a) Excitation spectra obtained for the pump-probe delays of 0.15 and 1.9 ps. In order to retrieve the nonequilibrium electronic temperature T_e for each case, the experimental data are fitted with a difference of the Fermi-Dirac distribution functions, $\Delta f = f(T_e) - f(T)$. (b) The temporal evolution of T_e. (c) The e-ph scattering times and corresponding values of the electron mean-free path obtained from the measured thermalization dynamics of the electronic system.

each case. We note that large-diameter MWCNTs are characterized as Fermi-liquid systems,[23] which justifies the use of the Fermi-Dirac distribution function, $f(T)$. The temporal evolution of the electronic temperature, T_e, is shown in Fig. 3(b). The dashed line represents the initial lattice temperature, $T = 380$ K, which remains constant during the relaxation of excited carriers.

The resulting e-ph scattering times, obtained within the thermalization approach, are shown in Fig. 3(c) along with the associated electron mean-free paths. The latter is found to be within 0.8 and 4 μm, which agrees well with the range of l inferred from the direct measurements of $\tau_{\text{e-ph}}$ (see Fig. 2). This agreement provides compelling evidence that the overall experimental uncertainty for measurements of the mean-free path is kept sufficiently below the absolute value of l.

In addition to the their potential relevance in understanding the nature of electron transport in MWCNTs, our findings indicate that the phonon-induced resistance to charge transport is strongly dependent on the applied voltage. In particular, we show that near the Fermi level ($V < 0.1$ eV) the ballistic travel of carriers is close to 4 μm, which is comparable to the nanotube length, whereas in high-current regime ($V \geqslant 0.3$ eV) l decreases to less than 1 μm.

This work was supported by Chemical Sciences, Geosciences and Biosciences Division, Office of Basic Energy Sciences, Office of Science, U.S. Department of Energy.

[1] A. Bachtold, C. Strunk, J. P. Salvetat, J. M. Bonard, L. Forro, T. Nussbaumer, and C. Schonenberger, Nature (London) **397**, 673 (1999).
[2] B. Q. Wei, R. Vajtai, and P. M. Ajayan, Appl. Phys. Lett. **79**, 1172 (2001).
[3] C. Schönenberger, A. Bachtold, C. Strunk, J.-P. Salvetat, and L. Forró, Appl. Phys. A: Mater. Sci. Process. **69**, 283 (1999).
[4] P. J. de Pablo, E. Graugnard, B. Walsh, R. P. Andres, S. Datta, and R. Reifenberger, Appl. Phys. Lett. **74**, 323 (1999).
[5] S. Frank, P. Poncharal, Z. L. Wang, and W. A. de Heer, Science **280**, 1744 (1998).
[6] A. Urbina, I. Echeverria, A. Perez-Garrido, A. Diaz-Sanchez, and J. Abellan, Phys. Rev. Lett. **90**, 106603 (2003).
[7] W. Yi, L. Lu, H. Hu, Z. W. Pan, and S. S. Xie, Phys. Rev. Lett. **91**, 076801 (2003).
[8] A. Kanda, K. Tsukagoshi, Y. Aoyagi, and Y. Ootuka, Phys. Rev. Lett. **92**, 036801 (2004).
[9] A. Bachtold, M. S. Fuhrer, S. Plyasunov, M. Forero, E. H. Anderson, A. Zettl, and P. L. McEuen, Phys. Rev. Lett. **84**, 6082 (2000).
[10] C. Berger, Y. Yi, Z. L. Wang, and W. A. de Heer, Appl. Phys. A: Mater. Sci. Process. **74**, 363 (2002).
[11] A. Bachtold, M. de Jonge, K. Grove-Rasmussen, P. L. McEuen, M. Buitelaar, and C. Schonenberger, Phys. Rev. Lett. **87**, 166801 (2001).
[12] H. J. Li, W. G. Lu, J. J. Li, X. D. Bai, and C. Z. Gu, Phys. Rev. Lett. **95**, 086601 (2005).
[13] Y. Qimin, W. Jian, Z. Gang, D. Wenhui, and G. Bing-Lin, Phys. Rev. B **72**, 155425 (2005).
[14] Z. Yao, C. L. Kane, and C. Dekker, Phys. Rev. Lett. **84**, 2941 (2000).
[15] J.-Y. Park, S. Rosenblatt, Y. Yaish, V. Sazonova, H. Ustunel, S. Braig, T. A. Arias, P. W. Brouwer, and P. L. McEuen, Nano Lett. **4**, 517 (2004).
[16] M. Zamkov, N. Woody, B. Shan, H. S. Chakraborty, Z. Chang, U. Thumm, and P. Richard, Phys. Rev. Lett. **93**, 156803 (2004).
[17] T. Hertel, R. Fasel, and G. Moos, Appl. Phys. A: Mater. Sci. Process. **75**, 449 (2002).
[18] NanoLab, Inc., 55 Chapel Street, Newton, MA 02458.
[19] Y. F. Chen and M. S. Fuhrer, Phys. Rev. Lett. **95**, 236803 (2005).
[20] T. Hertel and G. Moos, Phys. Rev. Lett. **84**, 5002 (2000).
[21] P. B. Allen, Phys. Rev. Lett. **59**, 1460 (1987).
[22] G. Moos, R. Fasel, and T. Hertel, J. Nanosci. Nanotechnol. **3**, 145 (2003).
[23] M. Zamkov, N. Woody, B. Shan, Z. Chang, and P. Richard, Phys. Rev. Lett. **94**, 056803 (2005).